https://doi.org/10.5194/gmd-2020-442
Preprint. Discussion started: 9 March 2021

Geoscientific Model Development Discussions
Open Access
EGU

A versatile method for computing optimized snow albedo from spectrally fixed radiative variables : VALHALLA v1.0

Florent Veillon [1,2], Marie Dumont [2], Charles Amory [1,3], and Mathieu Fructus [2]

[1]Laboratory of Climatology, Department of Geography, SPHERES, University of Liège, Liège, Belgium
[2]Université Grenoble Alpes, Université de Toulouse, Météo-France, CNRS, CNRM, Centre d'Etudes de la Neige, 38000 Grenoble, France
[3]Université Grenoble Alpes, CNRS, Institut des Géosciences de l'Environnement, 38000, Grenoble, France

Correspondence: Florent Veillon (fveillon@uliege.be)

Abstract. In climate models, the snow albedo scheme generally calculates only a narrowband or broadband albedo, which leads to significant uncertainties. Here, we present the Versatile ALbedo calculation metHod based on spectrALLy fixed radiative vAriables (VALHALLA, version 1.0), to optimize spectral snow albedo calculation. For this optimization, the energy absorbed by the snowpack is calculated by the spectral albedo model Two-streAm Radiative TransfEr in Snow (TARTES) and the spectral irradiance model Santa Barbara DISORT Atmospheric Radiative Transfer (SBDART). This calculation takes into account the spectral characteristics of the incident radiation and the optical properties of the snow, based on an analytical approximation of the radiative transfer of snow. For this method, 30 wavelengths, called tie points (tps), and 16 reference irradiance profiles are calculated to incorporate the absorbed energy and the reference irradiance. The absorbed energy is then interpolated for each wavelength between two tps with adequate kernel functions derived from radiative transfer theory for snow and the atmosphere. We show that the accuracy of the absorbed energy calculation primarily depends on the adaptation of the irradiance of the reference profile to that of the simulation (absolute difference < 1 $\mathrm{W\,m^{-2}}$ for broadband absorbed energy and absolute difference < 0.005 for broadband albedo). In addition to the performance in accuracy and calculation time, the method is adaptable to any atmospheric input (broadband, narrowband), and is easily adaptable for integration into a radiative scheme of a global or regional climate model.

1 Introduction

The solar irradiance is an important source of energy to snow and ice surfaces. Absorption of shortwave radiation strongly depends upon the physical properties of snow and atmospheric conditions. The high albedo of fresh snow crystals limits energy absorption by the snowpack while darker or old snow and glacial ice absorb more energy (Warren, 1982; Gardner and Sharp, 2010). The snowpack may also contain light absorbing particles (LAPs, McKenzie Skiles and Painter, 2018), leading to a decrease in albedo (Warren, 1982; Picard et al., 2009; Gardner and Sharp, 2010; Libois et al., 2013; Dumont et al., 2014). Besides, the optical properties of snow and ice strongly vary with the wavelength (e.g. ice refraction index of Warren and Brandt, 2008). The snow spectral albedo, defined as the fraction between reflected and incident solar energy for a given wavelength (Grenfell et al., 1994), is higher for near-ultraviolet (near-UV, 300–400 nm), visible (400-700 nm) and near-

https://doi.org/10.5194/gmd-2020-442
Preprint. Discussion started: 9 March 2021


Geoscientific Model Development Discussions

infrared (near-IR, 750–1400 nm) but is lower in the IR part of the solar spectrum (Warren, 1982; Gardner and Sharp, 2010). The changes in albedo with snow and ice properties play a major role in the melt-albedo feedback (Cess et al., 1991). An increase in temperature favours rapid metamorphism and melting of the snow cover, which leads to coarser snow grains and less reflective surface. More energy is then absorbed and made available for heating the snowpack, enhancing snow metamorphism and melting (e.g. Flanner and Zender, 2006). The solar zenith angle (SZA , valid for direct radiation) and atmospheric conditions (e.g. clouds, aerosols loads, water vapour column), determine the amount of energy reaching the surface of the snowpack. For example, clouds influence the proportion of solar radiation reaching the surface and contribute to total incident radiation by emitting longwave radiation (Wetherald and Manabe, 1988; Schneider et al., 2019). For realistic estimates of the energy balance and melt over snow and ice surfaces, accurate knowledge of a set of atmospheric and snowpack properties is thus required (Picard et al., 2012).

In addition to the above-mentioned requirements, accuracy in the estimation of the energy absorbed at the snow surface can be achieved through spectral calculation of the albedo but remains numerically expensive. This is usually overcome in most global and regional climate models by computing broadband or narrowband albedo to estimate the energy budget at the snow and ice surfaces. The broadband albedo is defined as the ratio between total reflected and total incident solar energy integrated across the entire solar spectrum, whereas the narrowband albedo is integrated over several spectral bands. These integrations however lead to a bias in the calculation of the snowpack albedo, which ultimately propagates in the computation of the surface energy and mass budgets.

To overcome these uncertainties while maintaining an adequate calculation time to remain competitive, new methods are developed. One of them, recently developed by van Dalum et al., 2019, effectively couples a spectral albedo model with a narrowband radiation scheme. This method (Spectral-to-NarrOWBand ALbedo module; SNOWBAL) allows the coupling of the radiative transfer model TARTES (Two-streAm Radiative TransfEr in Snow, Libois et al., 2013) with the European Centre for Medium-Range Weather Forecasts (ECMWF) radiation McRad scheme based on the shortwave Rapid Radiation Transfer Model (RRTMsw) embedded in RACMO2 (Mlawer et al., 1997; Clough et al., 2005; Morcrette et al., 2008; ECMWF, 2009) . They used 14 predefined representative wavelengths (RWs, for every 14 bands of RRTMsw) dependent on irradiance distribution and albedo within a spectral band to calculate spectral albedo on the entire solar spectrum. To determine the 14 RWs, a limited number of properties of the atmosphere are selected using a look-up table. They demonstrate that RWs primarily depend on the SZA, cloud content and water vapour. This method is tested on different types of snow and for clear-sky and cloudy atmospheric conditions, and represents broadband snow albedo with low uncertainties (<0.01). In van Dalum et al. (2020a, b), the SNOWBAL module is evaluated in RACMO2 over the Greenland ice sheet. This method can therefore be used on large surfaces while accurately representing the albedo of snow and ice. However, this SNOWBAL method is only adapted to albedo calculation within the RACMO2 model. Application of this method is, therefore, unusable for other atmospherics inputs. In addition, the impact of snow properties on the calculation are not fully taken into account since the RWs only vary with the atmospheric properties.

Here, we describe a detailed method for calculating the spectral albedo of snow based on the determination of spectrally fixed radiative variables VALHALLA (Versatile ALbedo calculation metHod based on spectrALLy fixed radiative vAriables, version

https://doi.org/10.5194/gmd-2020-442
Preprint. Discussion started: 9 March 2021

Geoscientific Model Development Discussions

1.0). This method maintains adequate accuracy of albedo values while reducing calculation time irrespective of the radiative transfer scheme used for the atmosphere. The proposed method takes advantage of the spectral characteristics of incident radiation and optical snow properties, based on the analytical approximation of the radiative transfer within the snowpack provided by Kokhanovsky and Zege (2004). These are calculated by TARTES combined with the model of spectral irradiance SBDART (Santa Barbara DISORT Atmospheric Radiative Transfer, Ricchiazzi et al., 1998). The results, obtained for a large number of simulations, are then compared with an albedo calculation by the TARTES-SBDART model at a spectral resolution of 1 nm. The sensitivity of the albedo calculations to both model inputs is also assessed. The results are finally compared with reference albedo calculations at different spectral resolutions.

2 Method

2.1 Radiative transfer model

The multilayer detailed snowpack model Crocus (Brun et al., 1989, 1992) represents the evolution of the snowpack due to its interactions with the atmosphere and the ground. In the original radiative transfer scheme of Crocus, the incident solar flux and albedo are calculated for 3 spectral bands. In the albedo calculation, only one or two layers of snow are accounted for. To improve the representation of the radiative transfer in snow, the spectral radiative transfer model TARTES has been implemented in Crocus (e.g. Tuzet et al., 2017). TARTES calculates spectral albedo in a multilayer snowpack when the physical properties of each layer and the angular and spectral characteristics of the radiation are known (Libois, 2014). It is based on the Kokhanovsky and Zege (2004) formalism for weakly absorbing media to describe the single-scattering properties of each layer and the delta-Eddington (Joseph et al., 1976) approximation to solve the radiative transfer equation. TARTES represents the snowpack as a stack of horizontal homogeneous layers. For calculation, physical properties of the snowpack (e.g., grain radius, grain shape, density, thickness, type of LAPs, LAPs concentration) and SZA for direct radiation (for diffuse radiation, SZA is fixed at 53°) are used as inputs. The grain size is characterized by the snow specific area (SSA; expressed in $\mathrm{m^2 kg^{-1}}$), defined as the ratio between the surface of the air-ice interface S and the ice mass (volume V) :

$$SSA = \frac{S}{V \varrho_{ice}} \tag{1}$$

with ϱ_{ice}, the volumetric mass of ice (917 $\mathrm{kg\ m^{-3}}$).

The grain shape is defined by 2 parameters: the asymmetry parameter g (dimensionless) and the absorption enhancement parameter B (dimensionless, Libois et al., 2013).

In Tuzet et al. (2017) and later studies, TARTES was used for calculations of radiative transfer with a spectral resolution of 20 nm. This resolution is the best compromise between the accuracy of radiation and calculation time, which is still very important, and makes this model configuration computationally expensive.

https://doi.org/10.5194/gmd-2020-442
Preprint. Discussion started: 9 March 2021

Geoscientific Model Development Discussions

2.2 SBDART

The model Santa Barbara DISORT Atmospheric Radiative Transfer (SBDART, Ricchiazzi et al., 1998) is used for radiative transfer calculation in clear-sky and cloudy conditions in the atmosphere. SBDART uses Discrete Ordinate Radiative Transfer (DISORT, Stamnes et al., 1988) to solve the radiative transfer equation in the atmosphere vertically homogeneous. This model is organized to permit up to 65 atmospheric layers and 40 radiation streams. The main input parameters used in this study are the aerosol optical depth (AOD), the cloud-layer optical depth (τ), the boundary layer aerosol type selector (IAER) and SZA. With these parameters, SBDART calculated direct and diffuse irradiance ($\mathrm{W\,m^{-2}}$) for each wavelength between 0.320 and 4.000 μm.

2.3 Absorbed energy by a snowpack

Kokhanovsky et al., 2018 demonstrate that the spectral albedo r of an homogeneous, optically infinite snowpack can be approximated by the following relationship :

$$r = exp(-u(\mu_0)\sqrt{(\alpha + f\tilde{\lambda}^{-m})l}) \tag{2}$$

where $u(\mu_0) = \frac{3}{7}(1+2\mu_0)$; μ_0 is the cosine of the solar zenith angle, $\alpha = \frac{4\pi\chi}{\lambda}$, where χ is the imagery part of the ice refractive index at the wavelength λ , f is the light absorbing particles concentration and l the size and shape of snow grain. $\tilde{\lambda}$ depend on the absorption coefficient of LAPs in snow $\chi_{abs}^{pol}(\lambda)$:

$$\chi_{abs}^{pol} = \chi_0 \tilde{\lambda}^{-m} \tag{3}$$

where $\chi_0 \equiv \chi_{abs}^{pol}(\lambda_0)$; $\tilde{\lambda} = \frac{\lambda}{\lambda_0}$;$\lambda_0 = 1\mu m$ and m is the absorption Angstrom coefficient.

Thus the first order of spectral albedo variations can be approximate as :

$$r(\lambda) \sim exp(-J\sqrt{\frac{n(\lambda)}{\lambda}}) \tag{4}$$

where $n(\lambda)$ is the imagery part of the ice refractive index at the wavelength λ and J which takes into account all snow and illumination properties and is constant with wavelength.

The fraction of absorbed energy in the snowpack f_p is thus related to the spectral albedo by the following relationship :

$$f_p(\lambda) = 1 - r(\lambda) \tag{5}$$

For the atmosphere, we use the Beer-Lambert law to express the first order spectral variations of the incoming solar radiation. The Beer-Lambert's law establishes a relationship between the radiation transmitted through a given media I and the incident irradiance I_0 at the wavelength λ. Let L be the thickness of the media and c_a the absorption coefficient. Then :

$$I(\lambda) = I_0(\lambda)\, exp(-c_a(\lambda)L) \tag{6}$$

Thus we assume that the spectral variations of the solar irradiance at the surface can be written :

$$I(\lambda) \sim E_{ref}(\lambda)\, exp(-D\sqrt{\frac{n(\lambda)}{\lambda}}) \tag{7}$$

https://doi.org/10.5194/gmd-2020-442
Preprint. Discussion started: 9 March 2021


Geoscientific Model Development Discussions

where E_{ref} is the total incident energy at the wavelength λ and D which takes into account all physical properties of the snowpack.

As a consequence, the absorbed energy by a snowpack for a given wavelength $E_{abs}(\lambda)$ can be approximated by :

$$E_{abs}(\lambda) \sim E_{ref}(\lambda)\, exp(-D\sqrt{\frac{n(\lambda)}{\lambda}})\, f_p(\lambda) \tag{8}$$

2.4 Calculation method

The calculation method is based on exact absorbed energy calculation at a limited number of wavelengths, hereafter referred to as tie points (tps), and interpolation between these wavelengths with the help of the general shape of the spectrum given in the equation above (Equation 8).

The method uses a reference irradiance profile with a spectral resolution of 1 nm. For each SZA value (varying between 10 and 80), a reference irradiance profile is calculated with SBDART. In total, 16 reference profiles were used (one set for clear-sky and partially cloudy conditions and the other one for full overcast conditions; see Section 2.5.2). These profiles are used to calculate a coefficient C between the broadband reference irradiance E_{ref} (integral of the reference profile) and broadband experience irradiance E_{exp}:

$$C_{b_i}^{b_{i+1}} = \frac{\int_{b_i}^{b_{i+1}} E_{exp}}{\int_{b_i}^{b_{i+1}} E_{ref}} \tag{9}$$

where b_i and b_{i+1} are the boundaries of the bands in which the model is providing the solar incident radiation. Here, b_i = 320 nm and b_{i+1} = 4000 nm.

For each tp, the absorbed energy and irradiance are calculated using TARTES-SBDART and used for determining the values of variables D and J.

Between two tie-points tp_n and tp_{n+1}, we assume that the absorbed energy can be approximated by :

$$E_{abs}(\lambda_{tp_n}^{tp_{n+1}}) = C_{b_i}^{b_{i+1}}\ E_{ref}(\lambda_{tp_n}^{tp_{n+1}})\, exp(-D_{tp_n}^{tp_{n+1}}\ \sqrt{\frac{n(\lambda_{tp_n}^{tp_{n+1}})}{\lambda_{tp_n}^{tp_{n+1}}}})\, (1 - exp(-J_{tp_n}^{tp_{n+1}}\ \sqrt{\frac{n(\lambda_{tp_n}^{tp_{n+1}})}{\lambda_{tp_n}^{tp_{n+1}}}})) \tag{10}$$

To determine these variables, which take into account all snow and illumination properties, an optimization by the least-square method is used. Indeed, D and J are mutually dependent.

In the context of optimization, variable D is written in :

$$G_{tp_n}^{tp_{n+1}} = exp(-D_{tp_n}^{tp_{n+1}}\ \sqrt{\frac{n(tp_n)}{tp_n}}) \tag{11}$$

with :

$$D_{tp_n}^{tp_{n+1}} = -log(\ G_{tp_n}^{tp_{n+1}}\ )\ \sqrt{\frac{tp_n}{n(tp_n)}} \tag{12}$$

https://doi.org/10.5194/gmd-2020-442
Preprint. Discussion started: 9 March 2021

Geoscientific Model Development Discussions

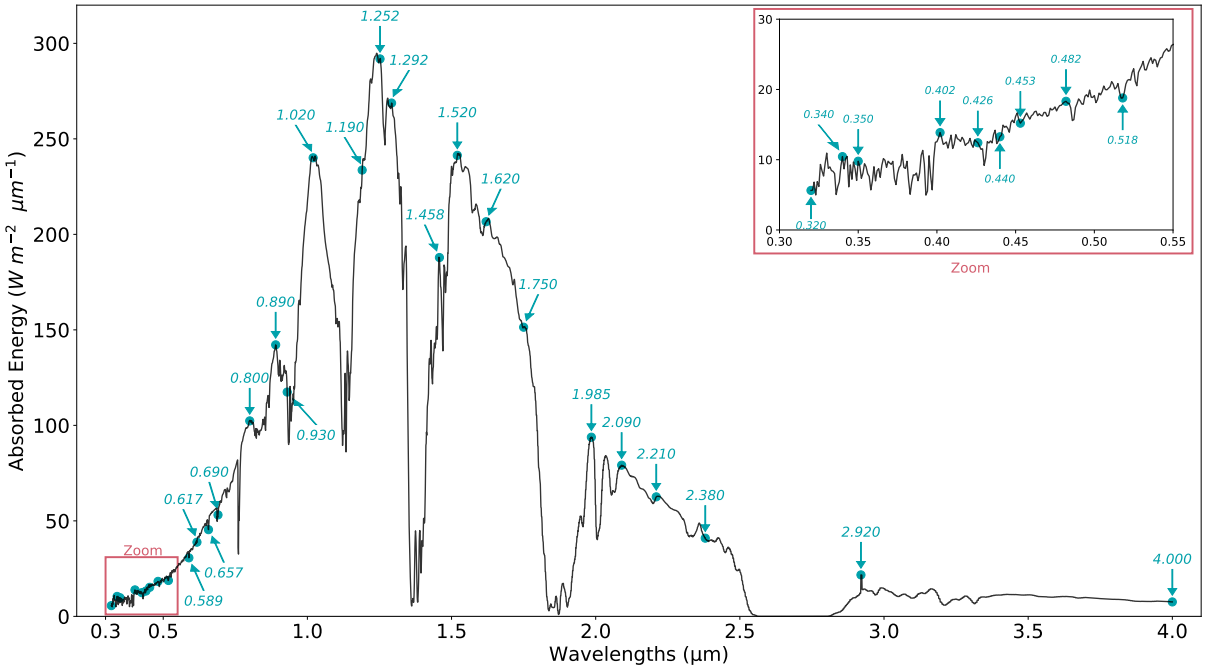

Figure 1. Spectral positions of tps on an example of absorbed energy profile by a snowpack without LAPs.

and J :

$$J_{tp_n}^{tp_{n+1}} = -log(\,1 - \frac{E_{abs_{tp_n}}}{C_{b_i}^{b_{i+1}}\, E_{ref_{tp_n}}}\, G_{tp_n}^{tp_{n+1}}\,) \sqrt{\frac{tp_n}{n(tp_n)}} \tag{13}$$

The optimization is realised on the variable $G_{tp_n}^{tp_{n+1}}$ and uses absorbed energy E_{abs} and total irradiance E_{ref} for tp_{n+1}.

$$\Delta_{tp_n}^{tp_{n+1}} = E_{abs_{tp_{n+1}}} - C_{b_i}^{b_{i+1}}\, E_{ref_{tp_{n+1}}}\, G_{tp_n}^{tp_{n+1}}\, (1 - exp(-J_{tp_n}^{tp_{n+1}} \sqrt{\frac{n(tp_{n+1})}{tp_{n+1}}})) \tag{14}$$

To find $G_{tp_n}^{tp_{n+1}}$ to make $\Delta_{tp_n}^{tp_{n+1}}$ as small as possible.

2.5 Numericals settings

2.5.1 Tie points

tps are reference wavelengths for absorbed energy and total irradiance. For all types of snow and cloud cover, a total of 30 tps is selected as a compromise between accuracy and computational time (Fig 1). The tp has been selected as the local maxima and minima of absorbed energy after several optimization tests (not shown).

https://doi.org/10.5194/gmd-2020-442
Preprint. Discussion started: 9 March 2021

Geoscientific Model Development Discussions

Table 1. Atmospheric parameters of reference irradiance profiles. Each irradiance profile is calculated for eight values of SZA and two values of τ. The other parameters are fixed in the SBDART model.

Cloud cover conditions	**Clear-sky and partially cloudy**	**Full overcast**
Solar zenith angle (°, SZA)	10 ; 20 ; 30 ; 40 ; 50 ; 60 ; 70 ; 80	
Boundary layer aerosol type (IAER)	2 - urban	
Aerosol optical depth (AOD)	0.07	
Cloud-layer optical depth (τ)	0.5	10
Integrated ozone concentration(atm-cm)	0.3	
Integrated water vapor amount ($\mathrm{g\,cm^{-2}}$)	0.35	
Surface altitude (km)	2.1	
Optical depth of each stratospheric aerosol layer	0.013	
Atmospheric profile	3 - Mid-Latitude Winter	

2.5.2 Reference irradiance profiles

To account for a representative set of atmospheric conditions, different reference irradiance profiles depending on SZA and cloud cover are chosen. These profiles are calculated by SBDART simulations with a spectral resolution of 1 nm for two cloud cover types. For simulations of clear-sky and partly cloudy conditions, reference irradiance profiles with values of τ equal to 0.5 are calculated. For simulations of full-overcast conditions, these profiles are calculated with a value of τ equal to 10 (Table 1).

2.5.3 SBDART settings

The main SBDART input parameters used in this study are the aerosol optical depth (AOD), cloud-layer optical depth (τ), boundary-layer aerosol type selector (IAER) and SZA (Table 2). These parameters have been chosen through preliminary experience plans and principal component analysis. Both aimed at determining a list of representative reduced experiences and parameters with the most pronounced influence on model outputs. For each value of the identified parameter and for each wavelength between 320 and 4000 nm, an irradiance profile is calculated.

2.5.4 TARTES settings

The main TARTES input parameters used in this study are the surface specific area (SSA) of the first layer of the snowpack, the snow water equivalent (SWE) for each layer of the snowpack and the LAPs concentration. We consider a snowpack with 3 layers of varying thickness and density (Table 3). These layers represent at most the first 20 centimeters of the snowpack, whose physical properties largely determine the albedo of the snow.The principal parameters on albedo calculation are the SSA of the first layer, the SWE of the first layers and the LAPs concentration of two first layers of the snowpack. We selected a wide range of SSA values (2 to 155 $\mathrm{m^2kg^{-1}}$) in order to cover most of the snow type found on Earth : 2 and 5 $\mathrm{m^2kg^{-1}}$ for

https://doi.org/10.5194/gmd-2020-442
Preprint. Discussion started: 9 March 2021

Geoscientific Model Development Discussions
Open Access
EGU

Table 2. Atmospheric parameters of simulations. Each irradiance profile is calculated for eight values of the SZA, five values of IAER, three values of the AOD and five values of τ (one for clear-sky conditions, three for partially cloudy conditions and one fore full-overcast conditions). The other parameters are fixed in the SBDART model.

Solar zenith angle (°, SZA)	10 ; 20 ; 30 ; 40 ; 50 ; 60 ; 70 ; 80				
Boundary layer aerosol type (IAER)	0 no boundary layer	1 rural	2 urban	3 oceanic	4 tropospheric
Aerosol optical depth (AOD)	0.01		0.07	0.14	
Cloud-layer optical depth (τ)	0	0.1	0.5	0.9	10
Integrated ozone concentration(atm-cm)	0.3				
Integrated water vapor amount ($\mathrm{g\,cm^{-2}}$)	0.35				
Surface altitude (km)	2.1				
Optical depth of each stratospheric aerosol layer	0.013				
Atmospheric profile	3 - Mid-Latitude Winter				

old snow, 42 and 82 $\mathrm{m^2kg^{-1}}$ for moderately old snow and 155 $\mathrm{m^2kg^{-1}}$ for new snow (Domine et al., 2007). SWE gives the mass of snow and is the product between thickness (t) and density (d). For pure snow (without LAPs), the SWE values are provided for the first three layers of the snowpack. For snow with LAPs, the SWE and LAPs concentration (for soot and dust) are provided for the first two layers of the snowpack. For layer 3 and layer 4, the values of all input parameters are fixed.

3 Results

In this section, we compare the simulated broadband absorbed energy resulting from VALHALLA for 30 tps with that obtained with TARTES-SBDART for the same spectral range between 320 and 4000 nm. We first analyse the impact of incident solar radiation, cloud cover conditions and snow properties on the errors in the estimated absorbed energy and albedo. The efficiency of the method is then compared to the TARTES-SBDART calculation for different spectral resolutions ranging from 1 nm (reference simulations) to 100 nm.

3.1 Sensitivity of the absorbed energy to input parameters

Figure 2 shows the sensitivity of the median error on the absorbed energy calculated by the method to the atmospheric and snowpack physical properties. The calculated energy for one simulation is compared to the reference absorbed energy, calculated by TARTES-SBDART at 1 nm resolution, for the same simulation and each SZA. Overall, the median error on the broadband absorbed energy calculated for all simulations decreases with increasing SZA. Concerning the atmospheric properties, the median error on absorbed energy exhibits a stronger sensitivity to τ than to AOD. The median errors are small for values of τ equal to 0.1, 0.5 and 10 (absolute difference < 1 $\mathrm{W\,m^{-2}}$) but remain larger for values equal to 0.0, 0.9 and 5.0 (e.g. median error = 3.6 $\mathrm{W\,m^{-2}}$ for τ = 5 and SZA = 10°). Errors are lower when using an adequate reference irradiance profile

https://doi.org/10.5194/gmd-2020-442
Preprint. Discussion started: 9 March 2021

Geoscientific Model Development Discussions
Open Access
EGU

Table 3. Snow properties of simulations. The spectral albedo is calculated for eight values of SZA and five values of SSA for the snowpack first layer. For snow without LAPs, the SWE values are provided for the first three layers of the snowpack.For snow with LAPs, the SWE and the light absorbing particles concentration (for soot and dust) are provided for the first two layers of the snowpack. For layer 3 (not true for snow without LAPs) and layer 4, the values of all input parameters are fixed.

	Solar zenith angle (SZA, °)	10 ; 20 ; 30 ; 40 ; 50 ; 60 ; 70 ; 80			
Layer 1	SSA ($m^2 kg^{-1}$)	2, 5, 42, 82, 155			
	SWE ($kg\,m^{-2}$)	1	4	15	
	Thickness (t, m)	t : 0.01	t : 0.02	t : 0.05	
	Density (d, kg m^3)	d : 100	d : 200	d : 300	
	Soot concentration ($ng\,g$)	0, 100, 200			
	Dust concentration($ng\,g$)	0, 25000, 50000			
Layer 2	SSA ($m^2 kg^{-1}$)	42			
	SWE ($kg\,m^{-2}$)	1	4	15	
	Thickness (t, m)	t : 0.01	t : 0.02	t : 0.05	
	Density (d, kg m^3)	d : 100	d : 200	d : 300	
	Soot concentration ($ng\,g$)	0, 100, 200			
	Dust concentration($ng\,g$)	0, 25000, 50000			
Layer 3	SSA ($m^2 kg^{-1}$)	42			
	SWE ($kg\,m^{-2}$)	1	4	12.5	15
	Thickness (t, m)	t : 0.01	t : 0.02	t : 0.05	t : 0.05
	Density (d, kg m^3)	d : 100	d : 200	d : 250	d : 300
	Soot concentration ($ng\,g$)	0, 100			
	Dust concentration($ng\,g$)	0, 25000			
Layer 4	SSA ($m^2 kg^{-1}$)	42			
	SWE ($kg\,m^{-2}$)	600			
	Thickness (t, m)	t : 2			
	Density (d, kg m^3)	d : 300			
	Soot concentration ($ng\,g$)	0			
	Dust concentration($ng\,g$)	0			

https://doi.org/10.5194/gmd-2020-442
Preprint. Discussion started: 9 March 2021

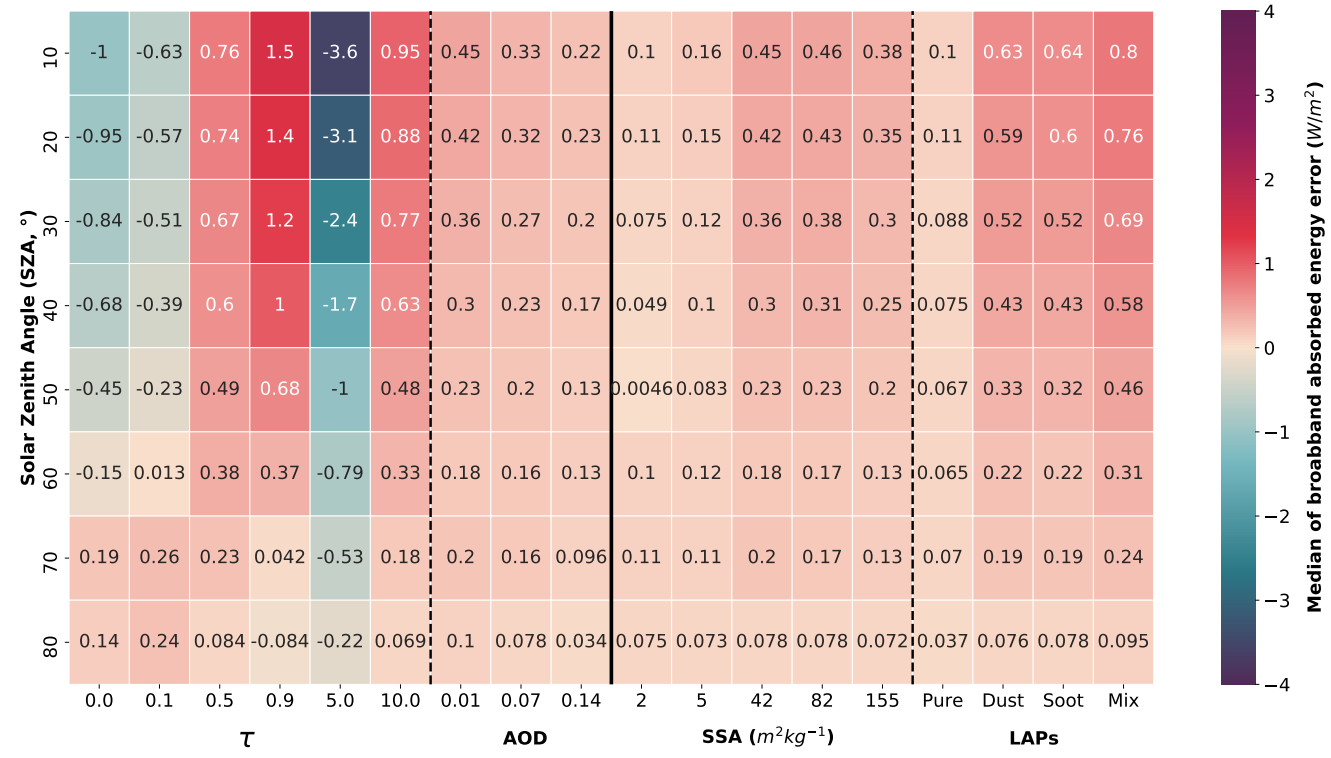

Figure 2. Median error of the broadband absorbed energy for varying SZA, the τ, the AOD, the SSA $\mathrm{m^2 kg^{-1}}$ and LAPs type. The median error on the broadband absorbed energy is calculated on the ensemble of all the simulations described in Section 5.c) and 5.d) using 30 *tps* using TARTES-SBDART at 1 nm resolution as reference.

(τ of simulation (τ_{simu}) equal to τ of reference (τ_{ref}), τ = 0.5 and 10) and the calculated absorbed energy is therefore very sensitive to τ (median errors between 1.5 and -3.6 $\mathrm{W\,m^{-2}}$). Regarding AOD, the median errors are small (absolute difference < 0.5 $\mathrm{W\,m^{-2}}$) and show little changes with τ. This demonstrates that AOD exerts a very small influence on the median error and thus on the calculation of the energy absorbed by the method. Concerning the properties of the snow cover, the SSA value of the first layer has little impact on the error on the absorbed energy. For the different SSA values, the median errors are small (absolute difference < 0.5 $\mathrm{W\,m^{-2}}$) and vary little depending on the value studied. The presence of LAPs in the snowpack leads to an increase in the median error (absolute difference < 1 $\mathrm{W\,m^{-2}}$) compared to pure snow (absolute difference < 0.1 $\mathrm{W\,m^{-2}}$). Overall the method slightly overestimates the energy absorbed by the snowpack (mostly positive errors). The error is not very sensitive to the physical properties of the snowpack and to the AOD. However, the error is very sensitive to τ of the simulations and thus to the τ chosen for the reference profile. The sensitivity to cloud conditions is investigated in more details in the next section.

https://doi.org/10.5194/gmd-2020-442
Preprint. Discussion started: 9 March 2021


Geoscientific Model Development Discussions

3.2 Sensitivity to cloud cover conditions

Figure 2 shows the median errors on the broadband absorbed energy for all the simulations. For each of them, the bias on the broadband absorbed energy is shown in Fig 3. Figure 3a,b. show the distribution of the biases in the broadband absorbed energy and the broadband albedo to SZA and τ. These biases are determined as the difference between the absorbed energy calculated by VALHALLA and TARTES-SBDART at 1 nm resolution. Overall, the biases of the absorbed energy decrease with SZA and the broadband albedo biases vary little with SZA. For simulations with a value of τ equal to 0.5 and 10 and each SZA value, an adequate reference irradiance profile is used ($\tau_{simu} = \tau_{ref}$). More than 75% of the errors are positive. The errors are low and range between -1 and 1.5 $\mathrm{W\,m^{-2}}$ with a median error of -0.76 and -0.95 $\mathrm{W\,m^{-2}}$ for τ equal to 0.5 and 10, respectively. For the simulations with a value of τ equal to 0, 0.1 and 0.9, the reference irradiance profile used has a τ value different from the simulations ($\tau_{simu} \neq \tau_{ref}$). For those with τ equal to 0 and 0.1, the biases are overall negative (for approximately 90% of the biases) and varies between -4 and 0.5 $\mathrm{W\,m^{-2}}$. For τ equal to 0.9, the biases of the absorbed energy are positive (for more than 95% of biases) and range between -0.5 and 2.8 $\mathrm{W\,m^{-2}}$.

Figure 3c,d. show the spectral variation of the reference absorbed energy calculated by TARTES-SBDART and that calculated by VALHALLA. The absorbed energy profiles presented are calculated for a simulation with two values of τ (0 and 10) between 320 and 4000 nm at 1 nm resolution. The spectral error of the absorbed energy is also calculated as the difference between the energy calculated by VALHALLA and TARTES-SBDART. For the simulation with τ equal to 0 (clear sky, Fig 3c), the majority of the errors are positive and are up to -9 $\mathrm{W\,m^{-2}\,\mu m}$). The higher errors are located at the wavelengths where the absorption is the highest (between 1 and 1.5 μm). For the one with τ equal to 10 (full overcast, Fig 3d), the method represents very well the absorbed energy (errors close to 0 $\mathrm{W\,m^{-2}\,\mu m}$). The use of an adequate reference irradiance profile ($\tau_{simu} = \tau_{ref}$) thus leads to a decrease of the error on the spectral and broadband absorbed energy, despite a slight overestimation of the energy absorbed by the method (positives errors). However, when $\tau_{simu} \neq \tau_{ref}$, the error on the absorbed energy is higher. When τ of the simulation is lower than τ of the reference profile ($\tau_{simu} < \tau_{ref}$), the absorbed energy is underestimated by the method (globally negative errors). When τ of the simulation is higher than τ of the reference profile $\tau_{simu} > \tau_{ref}$, the absorbed energy is overestimated by the method (positives errors). The biases of the absorbed energy are therefore very sensitive to τ of the simulations and therefore to the optical thickness chosen for the reference profile.

3.3 Sensitivity to snow physical properties

Figure 4a,b. show the distribution of the biases in broadband absorbed energy and albedo for varying SZA and SSA of the first layer of the snowpack. Broadband energy biases decrease with increasing SSA as the absolute absorbed energy is also decreasing. For an SSA equal to 2 $\mathrm{m^2kg^{-1}}$, the biases vary between -2 and 4 $\mathrm{W\,m^{-2}}$ as opposed to a variation of -1.5 to 1.5 $\mathrm{W\,m^{-2}}$ for an SSA equal to 155 $\mathrm{m^2kg^{-1}}$.

Figure 4c,d. show the spectral variation of the reference absorbed energy calculated by TARTES-SBDART and that calculated by the method. The absorbed energy profiles presented are calculated for a simulation with two extreme SSA values (5, representatives of old snow and 155 $\mathrm{m^2kg^{-1}}$ for new snow) between 320 and 4000 nm at 1 nm resolution. For these two

https://doi.org/10.5194/gmd-2020-442
Preprint. Discussion started: 9 March 2021

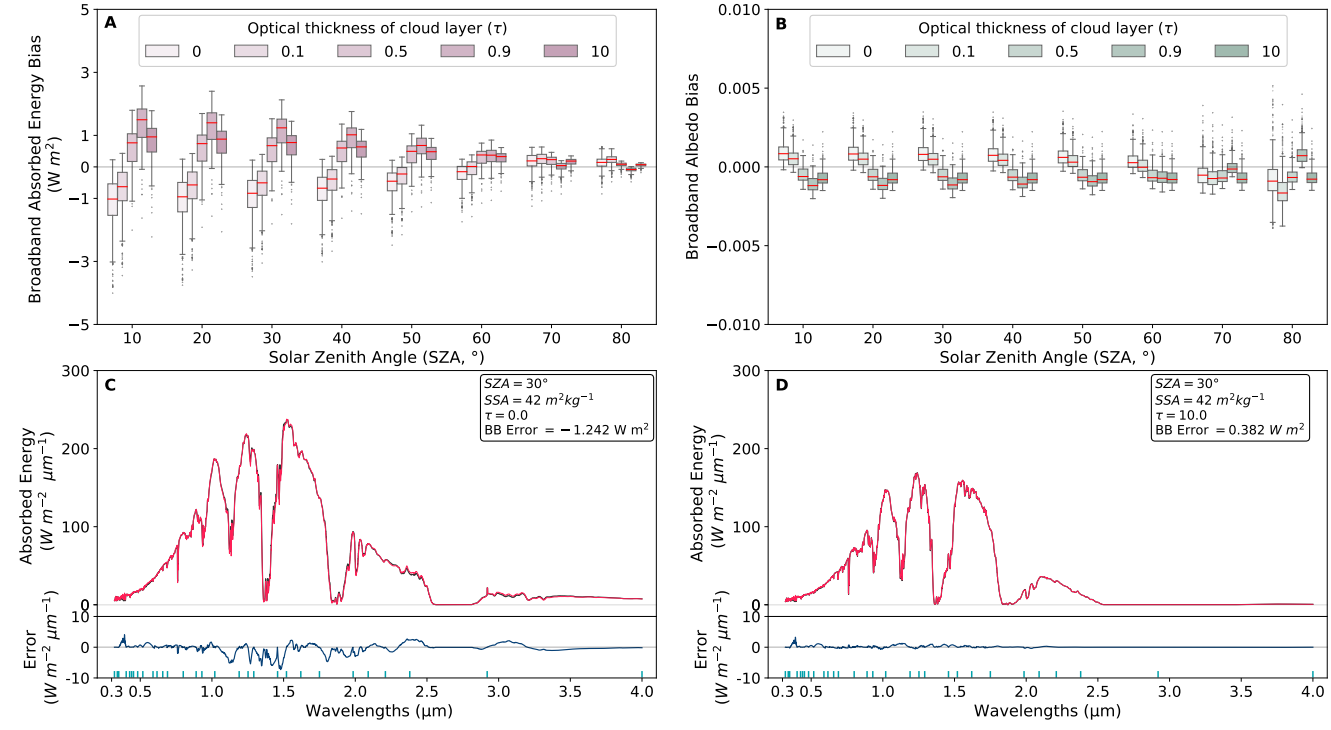

Figure 3. Bias on the broadband absorbed energy (A) and on the broadband albedo (B) as a function of the SZA and τ. The biases are calculated for all the simulations described 2.5.3. and 2.5.4., between the absorbed energy calculated by the method and the reference absorbed energy calculated by TARTES-SBDART. The red lines indicate the median (same as in Fig 2), the box shows the 25th to 75th percentiles and the whiskers show the 5th to 95th percentiles. Example of absorbed energy profiles by a snowpack without LAPs as a function of wavelength calculated for an SZA of 30° and a τ value of 0 (clear-sky, C) and a τ value of 10 (full overcast, D). The black lines represent the absorbed energy calculated by TARTES-SBDART at 1 nm resolution, and the red lines represent the absorbed energy calculated by VALHALLA. In blue, the errors on the absorbed energy for these same simulations as a function of wavelength. The green vertical lines represent the tps used in VALHALLA.

https://doi.org/10.5194/gmd-2020-442
Preprint. Discussion started: 9 March 2021

Geoscientific Model Development Discussions

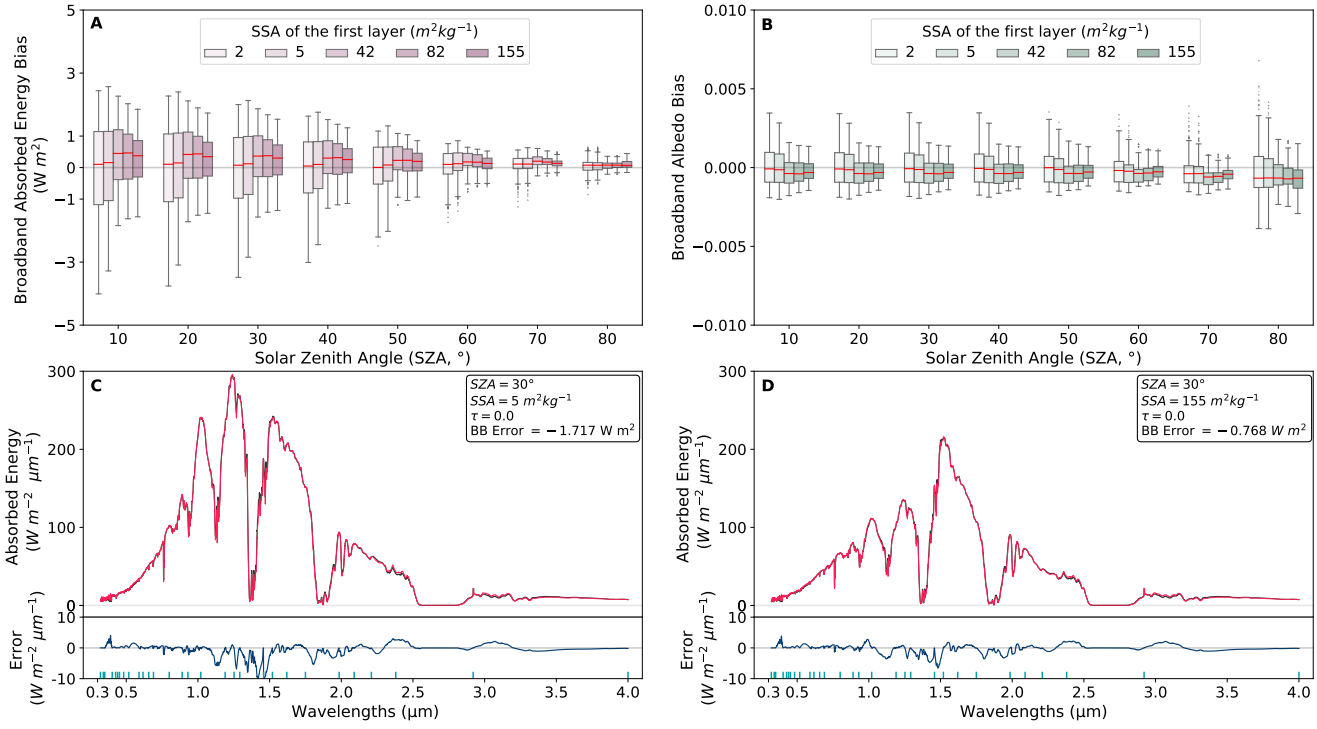

Figure 4. Bias on the broadband absorbed energy (A) and on the broadband albedo (B) as a function of the SZA and the SSA of the first layer (m^2kg^{-1}). The biases are calculated for all the simulations described 2.5.3. and 2.5.4., between the absorbed energy calculated by the method and the reference absorbed energy calculated by the TARTES-SBDART. The red lines indicate the median, the box shows the 25th to 75th percentiles and the whiskers show the 5th to 95th percentiles. Example of absorbed energy profiles by a snowpack without LAPs as a function of wavelength calculated for an SZA of 30° and an SSA value of 5 m^2kg^{-1} (old snow, C) and an SSA value of 155 m^2kg^{-1}(fresh snow, D). The black lines represent the absorbed energy calculated by TARTES-SBDART at 1 nm resolution, and the red lines represent the absorbed energy calculated by VALHALLA. In blue, the errors on the absorbed energy for these same simulations as a function of wavelength. The green vertical lines represent the tps used in VALHALLA.

simulations, the spectral errors of the absorbed energy are greater for an SSA value equal to 5 m^2kg^{-1} (up to -10 $W m^{-2} \mu m$), than for an SSA of 155 m^2kg^{-1} (> -8 $W m^{-2} \mu m$). The highest errors for these two simulations are located at the wavelengths where absorption is maximal (between 1 and 1.5 µm). When the snowpack is absorbing a large amount of energy, such as for low SSA, the biases on the spectral and broadband absorbed energy increase. The biases on the absorbed energy are therefore relatively sensitive to the SSA of the first layer of the snowpack and thus remain very sensitive to the absorbing properties of the snowpack.

https://doi.org/10.5194/gmd-2020-442
Preprint. Discussion started: 9 March 2021


Geoscientific Model Development Discussions

3.4 Sensitivity to LAPs

Figure 5a,b. show the distribution of the biases in broadband absorbed energy and albedo for various solar zenithal angles and LAPs contents. Broadband energy biases increase with the presence of LAPs in the snowpack. However, for pure snow, the biases are more negative than for snow with LAPs and the spread of the biases is greater (between -4 and 1.2 $\mathrm{W\,m^{-2}}$). For snow with dust or soot, the distribution of biases is very similar (between -1 and 2 $\mathrm{W\,m^{-2}}$) whereas for snow with a mix of dust and soot, the spread is larger (between -2 and 2.7 $\mathrm{W\,m^{-2}}$).

Figure 5c,d. show the spectral variation of the reference absorbed energy calculated byTARTES-SBDART and that calculated by VALHALLA. The absorbed energy profiles presented are calculated for a simulation with two LAPs concentration contained in the snowpack (a snowpack which contains 25000 $\mathrm{ng\,g^{-1}}$ of dust and a snowpack which contains a mix of 100 $\mathrm{ng\,g^{-1}}$ of soot and 50000 $\mathrm{ng\,g^{-1}}$ of dust) between 320 and 4000 nm at 1 nm resolution. LAPs being highly absorbent at the beginning of the spectrum (between 0.3 and 0.8 $\mu\mathrm{m}$, Warren, 1982), the most important errors are located in this wavelength range. For a snowpack containing a mix of LAPs (5d), the errors at the beginning of the spectrum are higher than for a snowpack containing only dust (5c). The presence of a mix of LAPs in the snowpack generates errors of up to -30 $\mathrm{W\,m^{-2}\,\mu m}$ against maximum errors of -20 $\mathrm{W\,m^{-2}\,\mu m}$ for the snowpack containing only dust. When the snowpack is absorbing a large amount of energy, such as with an important LAPs concentration, the biases on the spectral and broadband absorbed energy increase. The biases on the absorbed energy are therefore very sensitive to the LAPs content in the snowpack and thus remain very sensitive to the absorbing properties of the snowpack.

3.5 Comparison to constant spectral resolution calculations

For the same atmospherics and snow properties, the biais on the broadband albedo are computed by TARTES-SBDART for different constant spectral resolutions and compared with the results obtained by VALHALLA (Fig 6). To alleviate the effect of the very narrow (a few nm) absorption bands in the atmospheric irradiance profile, the broadband albedo is calculated between 320 and 4000 nm and then between 327 and 4000 nm. The method presents biases on the broadband albedo with absolute difference lower than 0.005 which are comparable to the bias obtained with resolutions lower or equal than 20 nm (reference resolution used at MétéoFrance in research activities). The method uses 30 tps against 184 wavelengths for a calculation at 20 nm resolution. However, for the same bias on the broadband albedo, the method thus uses six times fewer bands than a calculation at 20 nm resolution.

4 Discussions

We presented a calculation method VALHALLA for calculating absorbed energy and albedo based on a calculation of the main variables explaining the variations in absorbed energy using spectrally fixed radiative variables. We determined 30 tps, corresponding to the local minima and maxima of the absorbed energy at which the exact calculation of the absorbed energy is performed. In addition, we used 16 different reference irradiance profiles to interpolate between these tps. We evaluated the

https://doi.org/10.5194/gmd-2020-442
Preprint. Discussion started: 9 March 2021

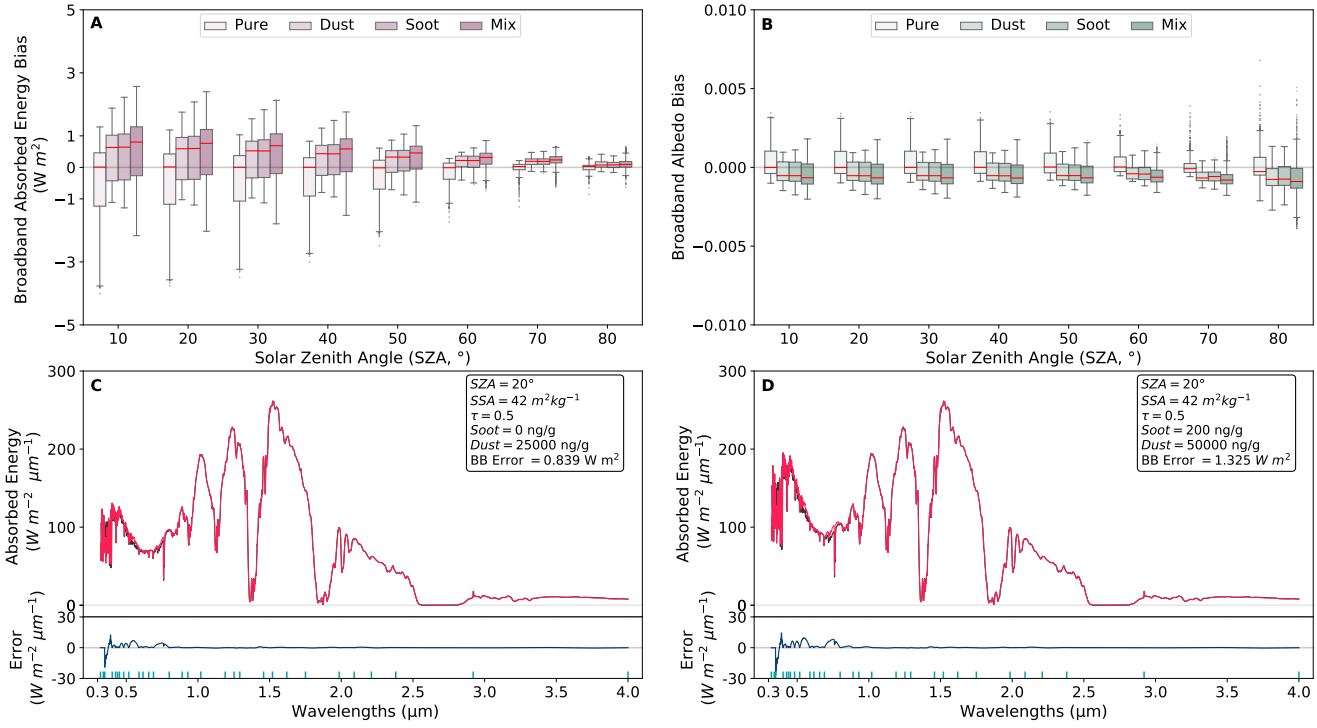

Figure 5. Bias on the broadband absorbed energy (A) and on the broadband albedo (B) as a function of the SZA and the LAPs content. The biases are calculated for all the simulations described sections 2.5.3. and 2.5.4., between the absorbed energy calculated by the method and the reference absorbed energy calculated by TARTES-SBDART. The red lines indicate the median, the box shows the 25th to 75th percentiles and the whiskers show the 5th to 95th percentiles. Example of absorbed energy profiles by a snowpack with LAPs as a function of wavelength calculated for an SZA of 30° for a snowpack which contains dust (C) and a mix of soot and dust (D). The black lines represent the absorbed energy calculated by TARTES-SBDART at 1 nm resolution, and the red lines represent the absorbed energy calculated by VALHALLA. In blue, the errors on the absorbed energy for these same simulations as a function of wavelength. The green vertical lines represent the tps used in VALHALLA.

https://doi.org/10.5194/gmd-2020-442
Preprint. Discussion started: 9 March 2021

Geoscientific Model Development Discussions

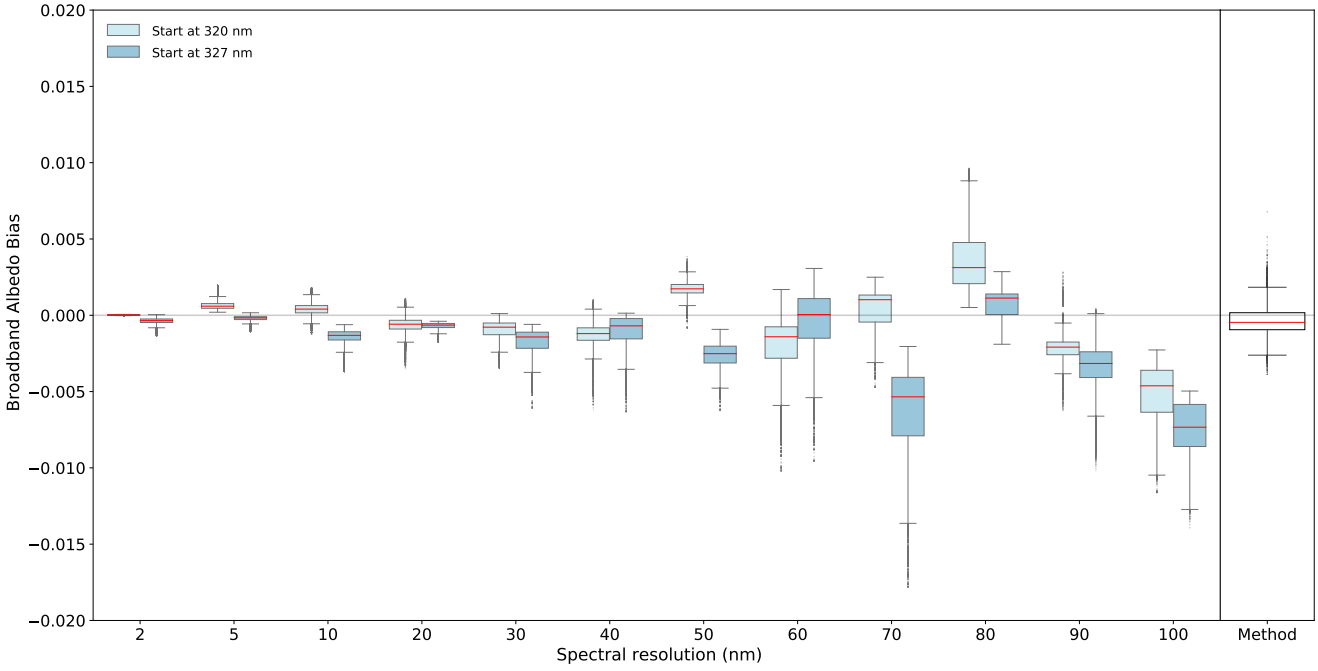

Figure 6. Errors on the broadband albedo for different constant spectral resolutions (left) and comparison with the errors of our method (right). For these resolutions, the broadband albedo is computed by TARTES-SBDART and is compared to the one computed for 1 nm resolution.

accuracy of the method for several atmospheric and snow properties that influence the amount of energy reaching the ground and snow albedo,such as τ, AOD, SSA and LAPs content. We have shown that absorbed energy and albedo errors due to the use of this method are small (absolute difference < 1 $\mathrm{W\,m^{-2}}$ for broadband absorbed energy and absolute difference < 0.005 for broadband albedo) and correspond to a factor 6 in terms of computation times compared to calculations made at 20 nm resolution.

We have shown that the absorbed energy calculated by VALHALLA is very sensitive to τ of the simulation and therefore to the use of an adequate reference irradiance profile. The use of a reference profile that is not adapted to the irradiance of the simulation ($\tau_{simu} \neq \tau_{ref}$) leads to a clear increase in the error on the absorbed energy. The irradiance provided by the method must, therefore, be as close as possible to the irradiance of the exact calculation to obtain a good representation of the absorbed energy. To reduce the uncertainties resulting from the method, a preliminary calculation of reference irradiance profiles adapted to each cloud condition could be initialized. Therefore, for all optical thickness values used in the simulations, the irradiance in the method can be adapted. The presence of LAPs in the snow cover leads to an increase in errors on the absorbed energy (especially at the beginning of the spectrum). With oscillations of the absorbed energy at the beginning of the spectrum, the method does not manage to converge towards a really accurate representation of the absorbed energy between two tps in the

https://doi.org/10.5194/gmd-2020-442
Preprint. Discussion started: 9 March 2021


Geoscientific Model Development Discussions

visible range. To reduce the uncertainties at the beginning of the spectrum and thus reduce the broadband error, it would be possible to increase the number of tps at the beginning of the spectrum. However, this would increase the calculation time. The choice of the number of tps is discussed later in this section. The other variables studied, such as the SZA and the SSA, appear to be less influential. The associated error evolves as a function of the amount of energy absorbed by the snowpack and is therefore driven by the absorbing factors such as the SZA and the SSA. The error on the absorbed energy, therefore, increases with a decrease in the solar angle and a decrease in the SSA value of the first layer of the snowpack. The choice of an adequate reference irradiance profile for the simulation globally determines the absorbed energy error calculated by VALHALLA. However, the choice of tps is also a determining factor in a good estimate of the energy absorbed by the method.

The tps were taken into account in the method (30 tps), leading to systematic errors for some wavelengths (e.g. 0.4 µm, Fig 3). Moreover, the tps correspond to local minima and maxima of the absorbed energy and represent a limit to the method. The optimal tps, more representative of the evolution of the absorbed energy, could be calculated and thus reduce the error on the calculation of this energy. An increase or a decrease in the number of tps could improve or alter the representation of the absorbed energy. Using a too large number of tps leads to a decrease in the calculated error but increases the calculation time, especially if the tp number is increased at the beginning of the spectrum to compensate for the oscillations of the absorbed energy when the snowpack contains LAPs. For a lower tp number, the oscillations at the beginning of the spectrum due to LAPs are not well represented by the method and this leads to a significant increase in the error. With the use of 15 tps, the error on the broadband albedo increases globally by a factor of 10 to 15 for snow containing LAPs. With 10 tps, the error increases by a factor of 25 and 50 for the same type of snow. The effect of LAPs on the absorbed energy is therefore poorly represented when the number of tp is too low. The use of 30 tp is, therefore, a good compromise between precision for snowpacks containing LAPs and calculation time.

van Dalum et al. (2019) developed a new albedo calculation method SNOWBAL based on the determination of a representative wavelength for each band of the model (14 atmospheric bands). These wavelengths are defined according to look-up tables as a function of the SZA, cloud content and water vapour. Through the use of these look-up tables, the method allows obtaining a good representation of the broadband albedo (<0.01). However, this narrowband computation method is not versatile and is only adapted to the RACMO2 model. The method presented is based on a spectral calculation of albedo versus a narrowband calculation in van Dalum et al. (2019). This allows obtaining the broadband albedo with absolute difference lower than 0.005 for VALHALLA against errors lower than 0.01 for SNOWBAL. However, VALHALLA uses 30 TPs versus 14 representative wavelengths for van Dalum et al. (2019). With the use of 15 tps, our method fails to converge to a good representation of the broadband albedo (increasing the error by a factor of 10 to 15). The use of more tps (30) is therefore necessary for an improved representation of the broadband albedo.

5 Conclusions

In climate models, energy fluxes are most often given for narrow and large spectral bands. The low spectral resolution of these fluxes therefore leads to uncertainties in the determination of radiative variables such as snow albedo that are key for

https://doi.org/10.5194/gmd-2020-442
Preprint. Discussion started: 9 March 2021


Geoscientific Model Development Discussions

energy exchanges at the surface. This study presents a new method VALHALLA for calculating the spectral albedo of snow based on the determination of key atmospheric and snow variables explaining variations in absorbed energy using spectrally fixed variables. For this method, tie points (tps) and reference irradiance profiles are calculated to incorporate the absorbed energy and the reference irradiance. The absorbed energy is then interpolated for each wavelength present between two tps with adequate kernel functions derived from radiative transfer theory for snow and the atmosphere.

For the different properties of the atmosphere and snow studied, the cloud-layer optical depth (τ) and the LAP content of the snow cover are the main variables influencing the calculation of the absorbed energy by the method. Indeed, when the value of τ of the simulation is equal to that of the reference irradiance profile, the method converges towards a value of absorbed energy close to that calculated as a reference. On the other hand, when this value is not equal to that of the reference profile, differences in absorbed energy are noticeable at certain wavelengths. For snowpacks containing LAPs, the method encounters difficulties in representing the variation in absorbed energy at the beginning of the spectrum and therefore generates significant differences in energy. For the other properties studied, the variables influencing the amount of energy absorbed by the snow, such as SZA and SSA, influence the calculation by the method when the reference irradiance profile is inadequate.

The VALHALLA method, therefore, determines the absorbed energy for all wavelengths between 320 and 4000 nm using 30 tps. This number of tps is necessary for a good representation of the absorbed energy when the snow contains LAPs. Despite an overestimation of the energy absorbed by the method, the results obtained with 30 tps are similar to the results of a TARTES-SBDART at 20 nm. This results in a reduction of the calculation time by a factor of 6 (30 tps versus 180 wavelengths). In addition to the performance in calculation time, the method is versatile and adaptable to any atmospheric input (broadband, narrowband).

In conclusion, the development of the method VALHALLA presented here allows a considerable reduction in calculation time while maintaining a good representation of the spectral albedo. One of the perspectives would be to integrate this method in a radiative scheme of a global or regional climate model in order to drastically reduce the calculation time and to largely improve the albedo calculation compared to more common broadband and/or narrowband calculations.

Code and data availability. The VALHALLA v1.0 development and data presented and described in this article (Veillon et al., 2020) is available for download at https://doi.org/10.5281/zenodo.4570565.

TARTES is freely avaibable on the website: http://pp.ige-grenoble.fr/pageperso/picardgh/tartes/. SBDART is freely available on the website: https://github.com/paulricchiazzi/SBDART.

Author contributions. FV, MD and MF started this project and developped the method. FV ran the simulations and wrote the first draft of the manuscript. FV, MD and CA performed the analysis . All authors discussed and revised the manuscript.

https://doi.org/10.5194/gmd-2020-442
Preprint. Discussion started: 9 March 2021

Geoscientific Model Development Discussions

Competing interests. The authors declare that they have no conflict of interests.

https://doi.org/10.5194/gmd-2020-442
Preprint. Discussion started: 9 March 2021

References

Brun, E., Martin, , Simon, V., Gendre, C., and Coleou, C.: An Energy and Mass Model of Snow Cover Suitable for Operational Avalanche Forecasting, Journal of Glaciology, 35, 333–342, https://doi.org/10.3189/S0022143000009254, 1989.

Brun, E., David, P., Sudul, M., and Brunot, G.: A numerical model to simulate snow-cover stratigraphy for operational avalanche forecasting, Journal of Glaciology, 38, 13–22, https://doi.org/10.3189/S0022143000009552, 1992.

Cess, R. D., Potter, G. L., Zhang, M. H., Blanchet, J. P., Chalita, S., Colman, R., Dazlich, D. A., Genio, A. D. D., Dymnikov, V., Galin, V., Jerrett, D., Keup, E., Lacis, A. A., Le Treut, H., Liang, X. Z., Mahfouf, J. F., Mcavaney, B. J., Meleshko, V. P., Mitchell, J. F. B., Morcrette, J. J., Norris, P. M., Randall, D. A., Rikus, L., Roeckner, E., Royer, J. F., Schlese, U., Sheinin, D. A., Slingo, J. M., Sokolov, A. S., Taylor, K. E., Washington, W. M., Wetherald, R. T., and Yagai, I.: Interpretation of Snow-Climate Feedback as Produced by 17 General Circulation Models, Science, 253, 888–892, https://doi.org/10.1126/science.253.5022.888, 1991.

Clough, S., Shephard, M., Mlawer, E., Delamere, J., Iacono, M., Cady-Pereira, K., Boukabara, S., and Brown, P.: Atmospheric radiative transfer modeling: a summary of the AER codes, Journal of Quantitative Spectroscopy and Radiative Transfer, 91, 233 – 244, https://doi.org/https://doi.org/10.1016/j.jqsrt.2004.05.058, 2005.

Domine, F., Taillandier, A.-S., and Simpson, W. R.: A parameterization of the specific surface area of seasonal snow for field use and for models of snowpack evolution, Journal of Geophysical Research: Earth Surface, 112, 2007.

Dumont, M., Brun, E., Picard, G., Michou, M., Libois, Q., Petit, J.-R., Geyer, M . Morin, S., and Josse, B.: Contribution of light-absorbing impurities in snow to Greenland's darkening since 2009, Nature Geoscience, 7, 509–512, https://doi.org/https://doi.org/10.1038/ngeo2180, 2014.

ECMWF: Part IV: Physical Processes, IFS Documentation, ECMWF, operational implementation 3 June 2008, 2009.

Flanner, M. G. and Zender, C. S.: Linking snowpack microphysics and albedo evolution, Journal of Geophysical Research: Atmospheres, 111, https://doi.org/https://doi.org/10.1029/2005JD006834, 2006.

Gardner, A. S. and Sharp, M. J.: A review of snow and ice albedo and the development of a new physically based broadband albedo parameterization, Journal of Geophysical Research: Earth Surface, 115, https://doi.org/10.1029/2009JF001444, 2010.

Grenfell, T. C., Warren, S. G., and Mullen, P. C.: Reflection of solar radiation by the Antarctic snow surface at ultraviolet, visible, and near-infrared wavelengths, Journal of Geophysical Research: Atmospheres, 99, 18 669–18 684, https://doi.org/10.1029/94JD01484, 1994.

Joseph, J. H., Wiscombe, W. J., and Weinman, J. A.: The Delta-Eddington Approximation for Radiative Flux Transfer, Journal of the Atmospheric Sciences, 33, 2452–2459, https://doi.org/10.1175/1520-0469(1976)033<2452:TDEAFR>2.0.CO;2, 1976.

Kokhanovsky, A., Lamare, M., Di Mauro, B., Picard, G., Arnaud, L., Dumont, M., Tuzet, F., Brockmann, C., and Box, J. E.: On the reflectance spectroscopy of snow, The Cryosphere, 12, 2371–2382, https://doi.org/10.5194/tc-12-2371-2018, 2018.

Kokhanovsky, A. A. and Zege, E. P.: Scattering optics of snow, Appl. Opt., 43, 1589–1602, https://doi.org/10.1364/AO.43.001589, 2004.

Libois, Q.: Evolution des propriétés physiques de neige de surface sur le plateau Antarctique. Observations et modélisation du transfert radiatif et du métamorphisme, Ph.D. thesis, Grenoble, 2014.

Libois, Q., Picard, G., France, J. L., Arnaud, L., Dumont, M., Carmagnola, C. M., and King, M. D.: Influence of grain shape on light penetration in snow, The Cryosphere, 7, 1803–1818, https://doi.org/10.5194/tc-7-1803-2013, 2013.

McKenzie Skiles, S. and Painter, T. H.: Assessment of Radiative Forcing by Light-Absorbing Particles in Snow from In Situ Observations with Radiative Transfer Modeling, Journal of Hydrometeorology, 19, 1397–1409, https://doi.org/10.1175/JHM-D-18-0072.1, 2018.

https://doi.org/10.5194/gmd-2020-442
Preprint. Discussion started: 9 March 2021

Mlawer, E. J., Taubman, S. J., Brown, P. D., Iacono, M. J., and Clough, S. A.: Radiative transfer for inhomogeneous atmospheres: RRTM, a validated correlated-k model for the longwave, Journal of Geophysical Research: Atmospheres, 102, 16 663–16 682, https://doi.org/10.1029/97JD00237, 1997.

Morcrette, J.-J., Barker, H. W., Cole, J. N. S., Iacono, M. J., and Pincus, R.: Impact of a New Radiation Package, McRad, in the ECMWF Integrated Forecasting System, Monthly Weather Review, 136, 4773–4798, https://doi.org/10.1175/2008MWR2363.1, 2008.

Picard, G., Arnaud, L., Domine, F., and Fily, M.: Determining snow specific surface area from near-infrared reflectance measurements: Numerical study of the influence of grain shape, Cold Regions Science and Technology, 56, 10 – 17, https://doi.org/https://doi.org/10.1016/j.coldregions.2008.10.001, 2009.

Picard, G., Domine, F., Krinner, G., Arnaud, L., and Lefebvre, E.: Inhibition of the positive snow-albedo feedback by precipitation in interior Antarctica, Nature Climate Change, 2, 795–798, https://doi.org/https://doi.org/10.1038/nclimate1590, 2012.

Ricchiazzi, P., Yang, S., Gautier, C., and Sowle, D.: SBDART: A Research and Teaching Software Tool for Plane-Parallel Radiative Transfer in the Earth's Atmosphere, Bulletin of the American Meteorological Society, 79, 2101–2114, https://doi.org/10.1175/1520-0477(1998)079<2101:SARATS>2.0.CO;2, 1998.

Schneider, T., Kaul, C. M., and Pressel, K. G.: Possible climate transitions from breakup of stratocumulus decks under greenhouse warming, Nature Geoscience, 12, 163–167, https://doi.org/10.1038/s41561-019-0310-1, 2019.

Stamnes, K., Tsay, S.-C., Wiscombe, W., and Jayaweera, K.: Numerically stable algorithm for discrete-ordinate-method radiative transfer in multiple scattering and emitting layered media, Appl. Opt., 27, 2502–2509, https://doi.org/10.1364/AO.27.002502, 1988.

Tuzet, F., Dumont, M., Lafaysse, M., Picard, G., Arnaud, L., Voisin, D., Lejeune, Y., Charrois, L., Nabat, P., and Morin, S.: A multilayer physically based snowpack model simulating direct and indirect radiative impacts of light-absorbing impurities in snow, The Cryosphere, 11, 2633–2653, https://doi.org/10.5194/tc-11-2633-2017, 2017.

van Dalum, C. T., van de Berg, W. J., Libois, Q., Picard, G., and van den Broeke, M. R.: A module to convert spectral to narrowband snow albedo for use in climate models: SNOWBAL v1.2, Geoscientific Model Development, 12, 5157–5175, https://doi.org/10.5194/gmd-12-5157-2019, 2019.

van Dalum, C. T., van de Berg, W. J., Lhermitte, S., and van den Broeke, M. R.: Evaluation of a new snow albedo scheme for the Greenland ice sheet in the regional climate model (RACMO2), The Cryosphere, 14, 3645–3662, https://doi.org/10.5194/tc-14-3645-2020, 2020a.

van Dalum, C. T., van de Berg, W. J., and van den Broeke, M. R.: Impact of updated radiative transfer scheme in RACMO2.3p3 on the surface mass and energy budget of the Greenland ice sheet, The Cryosphere Discussions, 2020, 1–30, https://doi.org/10.5194/tc-2020-259, https://tc.copernicus.org/preprints/tc-2020-259/, 2020b.

Warren, S. G.: Optical properties of snow, Reviews of Geophysics, 20, 67–89, https://doi.org/10.1029/RG020i001p00067, 1982.

Warren, S. G. and Brandt, R. E.: Optical constants of ice from the ultraviolet to the microwave: A revised compilation, Journal of Geophysical Research: Atmospheres, 113, https://doi.org/10.1029/2007JD009744, 2008.

Wetherald, R. T. and Manabe, S.: Cloud Feedback Processes in a General Circulation Model, Journal of the Atmospheric Sciences, 45, 1397–1416, https://doi.org/10.1175/1520-0469(1988)045<1397:CFPIAG>2.0.CO;2, 1988.